JOURNAL OF VIROLOGY, July 1997, p. 5560–5569 Vol. 71, No. 7
0022-538X/97/$04.00+0

The Range and Distribution of Murine Central Nervous System Cells Infected with the $\gamma_1$34.5$^-$ Mutant of Herpes Simplex Virus 1

NANCY S. MARKOVITZ,[1] DAVID BAUNOCH,[2] AND BERNARD ROIZMAN[1]*

The Marjorie B. Kovler Viral Oncology Laboratories[1] and the Department of Pathology,[2] the University of Chicago, Chicago, Illinois 60637

Received 6 February 1997/Accepted 8 April 1997

Wild-type herpes simplex virus 1 (HSV-1) multiplies, spreads, and rapidly destroys cells of the murine central nervous system (CNS). In contrast, mutants lacking both copies of the $\gamma_1$34.5$^-$ gene have been shown to be virtually lacking in virulence even after direct inoculation of high-titered virus into the CNS of susceptible mice (J. Chou, E. R. Kern, R. J. Whitley, and B. Roizman, Science 250:1262–1266, 1990). To investigate the host range and distribution of infected cells in the CNS of mice, 4- to 5-week-old mice were inoculated stereotaxically into the caudate/putamen with 3×10^5 PFU of the $\gamma_1$34.5$^-$ virus R3616. Four-micrometer-thick sections of mouse brains removed on day 3, 5, or 7 after infection were reacted with a polyclonal antibody directed primarily to structural proteins of the virus and with antibodies specific for neurons, astrocytes, or oligodendrocytes. This report shows the following: (i) most of the tissue damage caused by R3616 was at the site of injection, (ii) the virus spread by retrograde transport from the site of infection to neuronal cell nuclei at distant sites and to ependymal cells by cerebrospinal fluid, (iii) the virus infected neurons, astrocytes, oligodendrocytes, and ependymal cells and hence did not discriminate among CNS cells, (iv) viral replication in some neurons could be deduced from the observation of infected astrocytes and oligodendrocytes at distant sites, and (v) infected cells were being efficiently cleared from the nervous system by day 7 after infection. We conclude that the $\gamma_1$34.5$^-$ attenuation phenotype is reflected in a gross reduction in the ability of the virus to replicate and spread from cell to cell and is not due to a restricted host range. The block in viral replication appears to be a late event in viral replication.

The $\gamma_1$34.5 gene maps in the inverted repeats flanking the unique long sequence of the herpes simplex virus 1 (HSV-1) genome and therefore is present in two copies per genome. The gene encodes at least two functions. The first enables the virus to replicate in a variety of tissues but especially in the central nervous systems (CNS) of mice (13, 66). Thus, the PFU/50% lethal dose (LD_{50}) ratio of the mutant R3616 lacking the inverted repeats is $>10^6$. This compares with PFU/LD_{50} ratios of 2×10^2 to 4×10^2 obtained for virus HSV-1(F)R, in which the deleted sequences had been repaired, and for HSV-1(F), the wild-type parent virus, respectively (13). Attempts to recover virus from the brains of infected animals were either unsuccessful or yielded very small amounts of infectious virus (13, 66). Similar results were obtained with a mutant derived from a strain of HSV-2 and carrying deletions in the same genome domain (61, 62). The entire $\gamma_1$34.5 gene is required for expression of the virulence phenotype inasmuch as analyses showed that the virulence phenotypes of a series of mutants carrying identical in-frame deletions across the $\gamma_1$34.5 gene were attenuated (66a).

The second function expressed by the $\gamma_1$34.5 gene became apparent in in vitro studies of the $\gamma_1$34.5$^-$ mutants. In human cells infected with these mutants, protein synthesis was shut off prematurely independent of the shutoff of protein encoded by the U_L41 open reading frame (15, 54). Thus, although the double-stranded RNA-dependent protein kinase (PKR) is activated in human cells infected with wild-type virus, only in cells infected with $\gamma_1$34.5$^-$ virus is the α subunit of the translation initiation factor eIF-2 totally phosphorylated, accounting for the total shutoff of protein synthesis (12). The shutoff of protein synthesis was coincident with or subsequent to the onset of viral DNA synthesis and resulted in viral yields 10- to 100-fold lower than those of wild-type virus (14, 15). This function of the $\gamma_1$34.5 gene was mapped to the 3′ terminal 60 codons. It is of significance that this domain of the $\gamma_1$34.5 gene is homologous to the corresponding domain of a set of genes known by the acronym GADD34 (growth arrest and DNA damage). Indeed, substitution of the carboxyl terminus of $\gamma_1$34.5 with that of MyD116, the murine homolog of GADD34, restores protein synthesis but not the virulence phenotype of the $\gamma_1$34.5$^-$ mutants (25, 66b). Recently, one puzzle related to the $\gamma_1$34.5 gene has been at least in part solved. Detailed evidence reported elsewhere indicates that the $\gamma_1$34.5 protein binds protein phosphatase 1α and redirects its function to dephosphorylate eIF-2α (26).

Less is known about the mechanism through which the virulence phenotype of the $\gamma_1$34.5 gene is expressed. As the next step in the evaluation of the potential mechanisms responsible for the avirulent phenotype of the mutants with $\gamma_1$34.5 deleted, it was important to define the host range of the $\gamma_1$34.5$^-$ mutant in the CNS. Specifically, we were interested in the distribution and identity of the CNS cells infected by a small volume of $\gamma_1$34.5$^-$ virus administered in a specific, highly reproducible manner into the CNS of mice. In the series of experiments reported here, the $\gamma_1$34.5$^-$ mutant R3616 was stereotaxically injected into the neostriatum of 4- to 5-week-old mice and semiserial sections of paraffin-embedded brains harvested at 3, 5, or 7 days after infections were subjected to immunohisto-

* Corresponding author. Mailing address: The Marjorie B. Kovler Viral Oncology Laboratories, University of Chicago, 910 E. 58th St. Chicago, IL 60637. Phone: (773) 702-1898. Fax: (773) 702-1631. E-mail: bernard@Kovler.uchicago.edu.

chemical analysis to determine both the location and identity of infected cells.

As has been reported in numerous studies, wild-type HSV-1 spreads rapidly and efficiently along neuroanatomically defined pathways causing widespread infections throughout the CNS. HSV-1 infection is not confined to neurons; the virus has been reported to infect a variety of glial cells of the CNS (4, 10, 17, 30, 48, 52, 63, 65). Given the wealth of data on the behavior of wild-type viruses in the CNS, our studies focused entirely on R3616. Our results indicate that (i) R3616 caused limited tissue damage and cell loss at the site of infection, (ii) R3616 was capable of very limited spread within the CNS to distant sites, presumably through axonal transport but also through the cerebrospinal fluid (CSF) within the cerebral ventricles, (iii) the virus did not appear to discriminate between neurons, astrocytes, oligodendrocytes, and ependymal cells, (iv) the presence of infected oligodendrocytes and astrocytes at sites distal to the site of infection suggested that R3616 was able to replicate in neurons at very low levels, (v) the number of cells infected with R3616 peaked near day 5, and (vi) cells infected by R3616 were being efficiently cleared from the nervous system as evidenced by the decrease in the number and distribution of infected cells by day 7 after infection. The point to be stressed is that infection with the $\gamma_1$34.5$^-$ mutant would be best described as lethargic.

MATERIALS AND METHODS

Viruses. HSV-1(F) is the prototype HSV-1 strain used in this laboratory (18). The construction and relevant properties of the R3616 mutant generated by 1-kbp deletions from both copies of the $\gamma_1$34.5 gene of HSV-1(F) were reported elsewhere (13). For administration to the mouse CNS, an R3616 viral stock was diluted 1:30 in sterile phosphate buffered saline [PBS(A)]. To measure the amount of virus actually delivered to each mouse, four samples of 1 μl each were collected from the needle assembly at intervals during the course of the experiment and titers were determined. The inoculum size ranged from 2.1×10^5 to 4.3×10^5 PFU (average, 3.2×10^5 PFU).

CNS marker solution. A sterile solution of 2% methyl cellulose in PBS(A) and India ink served two purposes. First, it permitted macroscopic verification that the injections were centered in the caudate/putamen (neostriatum) prior to extensive histological tissue processing. Second, sections through the caudate/putamen of the mouse injected with the marker solution served as negative controls for immunohistochemical analysis.

Intracranial inoculation of virus. Male 4- to 5-week-old CBA/J mice were anesthetized with a mixture of ketamine and acepromazine (12 mg and 0.31 mg, respectively, per 100 g of body weight) injected intraperitoneally. The skull surrounding the bregma was exposed by a small incision through the skin, and a hole through the skull over the neostriatum was made with a dental drill equipped with a 0.75-mm-diameter burr. The head of the mouse was positioned into a Kopf stereotaxic apparatus fitted with a mouse adapter. The pitch of the bite bar remained set at 2 units, nose down from zero, for all mice. The needle assembly used for injection of the virus or marker solution consisted of a 30-gauge needle attached to a 50-μl Hamilton syringe (1705) advanced by a Hamilton repeating dispenser. The needle assembly was zeroed, positioned over the burr hole (0.4 to 1.0 mm anterior and 1.7 to 1.9 mm lateral to the bregma), and lowered to a depth of 3 mm ventral to the surface of the skull. A 1-μl bolus of virus or marker solution was injected and left undisturbed for at least 2 min before the needle was retracted. The burr hole was then sealed with bone wax, and the incision was closed with a wound clip. Mice were individually ear tagged, maintained in an incubator, and monitored until mobile. These procedures were approved by the University of Chicago Institutional Animal Care and Use Committee.

Fixation and sectioning. At 3, 5, or 7 days after infection, mice were given a lethal dose of pentobarbital sodium (Nembutal) intraperitoneally (5 mg/mouse) and, when areflexic, were quickly sacrificed by intracardiac perfusion of PBS(A) wash followed by 10% formalin. Brains were postfixed in 10% formalin overnight, sectioned grossly into four blocks in the transverse plane, dehydrated in an ascending series of alcohol to 100%, cleared in xylene, and paraffin embedded. Twenty 4-μm serial sections were collected at 320-μm intervals extending rostrally from the olfactory bulbs to the level of the locus coeruleus caudally. The interval between sections in a specific treatment series was therefore 320 to 480 μm.

Antibodies. Rabbit polyclonal antibody to HSV (PU086-UP; Biogenex, San Ramon, Calif.) was used at a dilution of 1:80. The manufacturer reported that the serum reacts with viral proteins and glycoproteins and does not discriminate between HSV-1 and HSV-2 antigens. Neurons were identified by their reactivity with mouse monoclonal antibody A60 generated against the neuron-specific nuclear protein Neu-N (51), a kind gift from Richard J. Mullen. Astrocytes were identified by reacting the brain sections with a rabbit polyclonal antibody generated against GFAP (Z0334; Dako Laboratories, Carpinteria, Calif.), whereas oligodendrocytes were identified with a rabbit polyclonal antibody generated against S-100 (Z0311; Dako Laboratories). The monoclonal antibodies CL28 to U_S11 and H114 to α4 (Goodwin Institute, Plantation, Fla.) were described elsewhere (1, 57). The monoclonal antibody to gC was obtained from the Goodwin Institute.

Immunohistochemistry. Mounted sections were baked, cleared in xylene, and hydrated through a descending alcohol series to distilled water. After microwave antigen retrieval, endogenous peroxidase activity was blocked by treating the sections with 3% hydrogen peroxide in methanol for 20 min. Two tissue sections at each level were then reacted overnight at 4°C with PU086-UP antibody. One slide from each sample was reacted in a similar fashion with normal rabbit serum immunoglobulin (Ventana Medical Systems, Tucson, Ariz.). The immunohistochemical staining was done on a Gen^{II} system (Ventana Medical Systems) which utilizes an indirect strepavidin biotin conjugated with horseradish peroxidase for detecting the immunocomplex and diaminobenzidine as the substrate for localization. For single-label analyses, sections reacted with PU086-UP antibody only were counterstained with hematoxylin, dehydrated though an ascending alcohol series, cleared, and mounted. A positive reaction to viral antigens was readily detected by the accumulation of a brown reaction product mainly within the nucleus of the cell.

To identify the infected cell type, sections neighboring those containing cells with viral antigens were then subjected to a double-labeling procedure which was identical to that used for PU086-UP staining alone but which had the following additional steps. Sections were washed briefly in APK wash solution (Ventana Medical Systems) and reacted overnight with the second antibody (1:200 dilution of A60, 1:800 dilution of anti-GFAP, or 1:800 dilution of anti-S-100). The immunohisochemical staining done on the Ventana Gen^{II} system used an indirect strepavidin biotin system conjugated with alkaline phosphatase for detecting the cell-type-specific immunocomplex and a fast red substrate for localization. Immunostained sections were then counterstained with hematoxylin, dehydrated though an ascending alcohol series, cleared, and mounted. Thus, for sections which were double labeled, the HSV-infected cells were identified by the accumulation of a brown reaction product mainly within the nucleus. All antibodies to cell-specific antigens stained the nucleus (neurons) or cytoplasm (astrocytes and oligodendrocytes) red.

Microscopy. All sections were viewed and photographed with Zeiss microscopes. Cells were judged to be double labeled if the section also contained uninfected cells labeled only with the cell-specific marker. The neuroanatomical nomenclature used is in accordance with Franklin and Paxinos (23).

RESULTS

The reactivity of the anti-HSV polyclonal antibody. We have selected the commercial anti-HSV antibody PU086-UP because of its widespread use for the identification of viral antigens in histological sections. To verify the manufacturer's claims and to ascertain the range of antigens reacting with this rabbit polyclonal antibody, confluent rabbit skin cells were either mock infected or exposed to 10 PFU of HSV-1(F) per cell. The cells were harvested at 26 h after infection, solubilized, and subjected to electrophoresis in a denaturing 12% polyacrylamide gel, and then they were transferred to nitrocellulose, blocked, and reacted with polyclonal rabbit antibody PU086-UP or with monoclonal antibodies to U_S11, α4, and gC and the appropriate secondary antibody. The protein bands were visualized by using nitroblue tetrazolium and 5-bromo-4-chloro-3-indolylphosphate as chromogens. The results (Fig. 1) show that antibody PU086-UP reacted with a wide range of viral antigens. These included α proteins exemplified by the product of the α4 gene and γ_2 virion structural proteins exemplified by the comigration of bands reactive with gC and U_S11 protein with bands reactive with PU086-UP (Fig. 1, lanes 2 and 4). Polyclonal rabbit antibody PU086-UP appears to exhibit a high level of specificity consistent with its failure to react with histologic sections from uninoculated mouse brain tissues, as described below.

Location and effect of injection. For the purpose of orientation, a composite photograph of Zeiss LSM microscopic images of HSV-1-immunostained sections at 320- to 480-μm intervals are shown in Fig. 2. The injection site of virus or the marker solution was in a relatively large nucleus, the caudate/

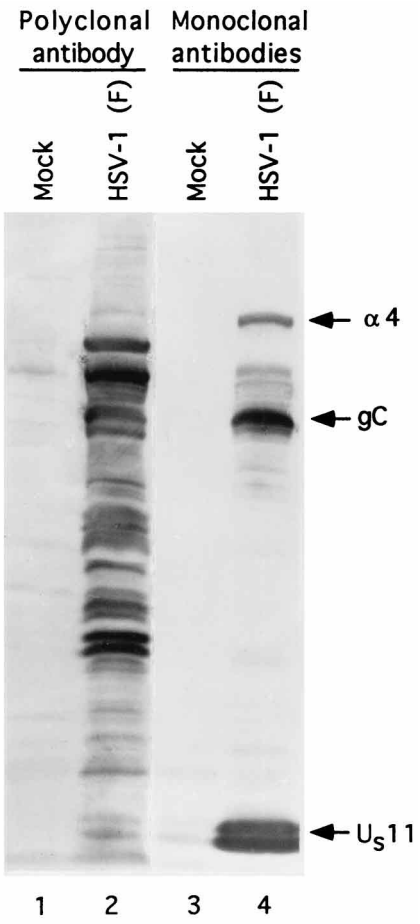

FIG. 1. Photograph of immunoblots of electrophoretically separated lysates of rabbit skin cells harvested at 26 h after infection or mock infection and probed with the PU086-UP polyclonal rabbit antibody (1:80; lanes 1 and 2) or sequentially with monoclonal antibodies to α4 (1:300), gC (1:500), and U_S11 (1:500; lanes 3 and 4).

putamen, in the forebrain of the mouse. The caudate/putamen, or neostriatum, extends hundreds of micrometers along the rostrocaudal axis and is visible in sections 4 to 7 of Fig. 2. The site of the injection is indicated in section 6. In order to differentiate the cytotoxic effects of the pressure of injection from those caused by virus on the tissue surrounding the injection site, we examined the appropriate sections from brains injected with either virus or marker suspensions. In sections from a mouse which received an injection of the marker suspension, at three days after injection there was minimal tissue disruption, low levels of cellular infiltration, and an expected increase in GFAP staining characteristic of the astrocytic reaction to a 3-day-old stab wound (Fig. 3a). The histologic sections showed no indications of significant cell loss or, as expected, of immunostaining with the PU086-UP antibody.

In contrast, sections through the site of R3616 injection showed increased tissue disruption and cellular infiltration, marked cell loss, and perivascular cuffing (Fig. 3b and c; Fig. 4h to j). Immunostaining with the PU086-UP antibody revealed the presence of diffuse viral antigen and a large number of infected cells distributed at varying distances within the neostriatum. In some levels of the brain, ependymal cells lining the cerebral ventricles (Fig. 3d and e) were also immunostained, suggesting that some of the virus may have escaped the neostriatum and entered the cerebral ventricles.

Distal distribution of infected cells. In the brains of mice injected with R3616, HSV-infected cells were detected in large numbers at the site of infection and in smaller numbers in many nuclei distal to the injection site (Table 1). The majority of infected cells were found in the amygdalopiriform transition area, the cingulate and adjacent motor cortices, the internal capsule, and the amygdala (Fig. 3i, j, k, and l; Fig. 4g and k to m; Table 1). A smaller number of infected cells were found in the lateral septal nuclei, locus coeruleus, dorsal raphe, and substantia nigra (Fig. 3f and g; Fig. 4a to f) and in the anterior olfactory cortex and fimbria (data not shown). The majority of these regions—motor and cingulate cortices (Fig. 3k), nuclei of the amygdala (Fig. 3i, j, and l; Fig. 4g and k to m), substantia nigra (Fig. 4e and f), and dorsal raphe (Fig. 4c and d)—contain neurons which extend their axons into the neostriatum (3, 19, 24, 27, 28, 32, 39–41, 44, 55, 60). The ability of HSV to infect and to be transported retrograde through the axons to the neuronal nucleus has made it an effective agent for tracing the connections of neurons within the brain (7, 8, 17, 29, 34, 35, 53, 64). Thus, with respect to the results of these studies, it is reasonable to propose that the axons or axon terminals were infected in the neostriatum and thus their nuclei, located in distant regions of the brain, were identified on the basis of the presence of viral antigens.

Temporal differences in the distribution and number of infected cells. Table 1 summarizes the number and distribution of immunolabeled cells found in diverse regions throughout the brains of mice injected with R3616 and sacrificed on day 3, 5, or 7 after injection. A comparison of the relative numbers of infected cells found in specific regions in each brain revealed the following. (i) The number of infected cells at the injection site and elsewhere in the neostriatum was lower in the mouse brain harvested on day 7 than in that harvested on day 3 or 5. Inasmuch as at this time there was also an associated increase in tissue damage and cell loss in this region of the brain (Fig. 3g and h), it is reasonable to conclude that the decrease in the number of labeled cells was due to the death of infected cells and their subsequent removal by the immune system. (ii) The number of infected cells found in distal regions such as the amygdala, amygdalopiriform transition area, and cortical regions increased between days 3 and 5. However, on day 7 after infection, no infected cells were detected in the amygdalopiriform transition area or cortical regions, while infected cells in the amygdala appeared to lack discrete boundaries and vacuoles were observed in the surrounding tissue (data not shown). Thus, the absence or decrease of infected cells may be explained by immune clearance by day 7, as was observed at the site of injection. Due to the inherent difficulty of delivering an injection to precisely the same location in the brain of a mouse, we cannot rule out the possibility that small shifts in the location of the injection could account for these differences in infected cell number and location. However, it should be stressed that the stereotaxic coordinates for the injection sites for these mice varied little, i.e., ±0.1 mm along the anterior-posterior plane and ±0.05 mm along the medial-lateral axis. (iii) Infected ventricular ependymal cells were present in the brains of mice sacrificed on days 3 and 5 (Fig. 3d and e). However, 7 days after infection, ependymal cells were largely absent from the lateral ventricles (Fig. 3f and g) (49). The absence of this ependymal cell layer suggests that by day 7 the majority of these cells had been infected, while far fewer ependymal cells had been infected by days 3 or 5. This increase in the proportion of infected ependymal cells implies that either a larger fraction of the inoculum initially gained access

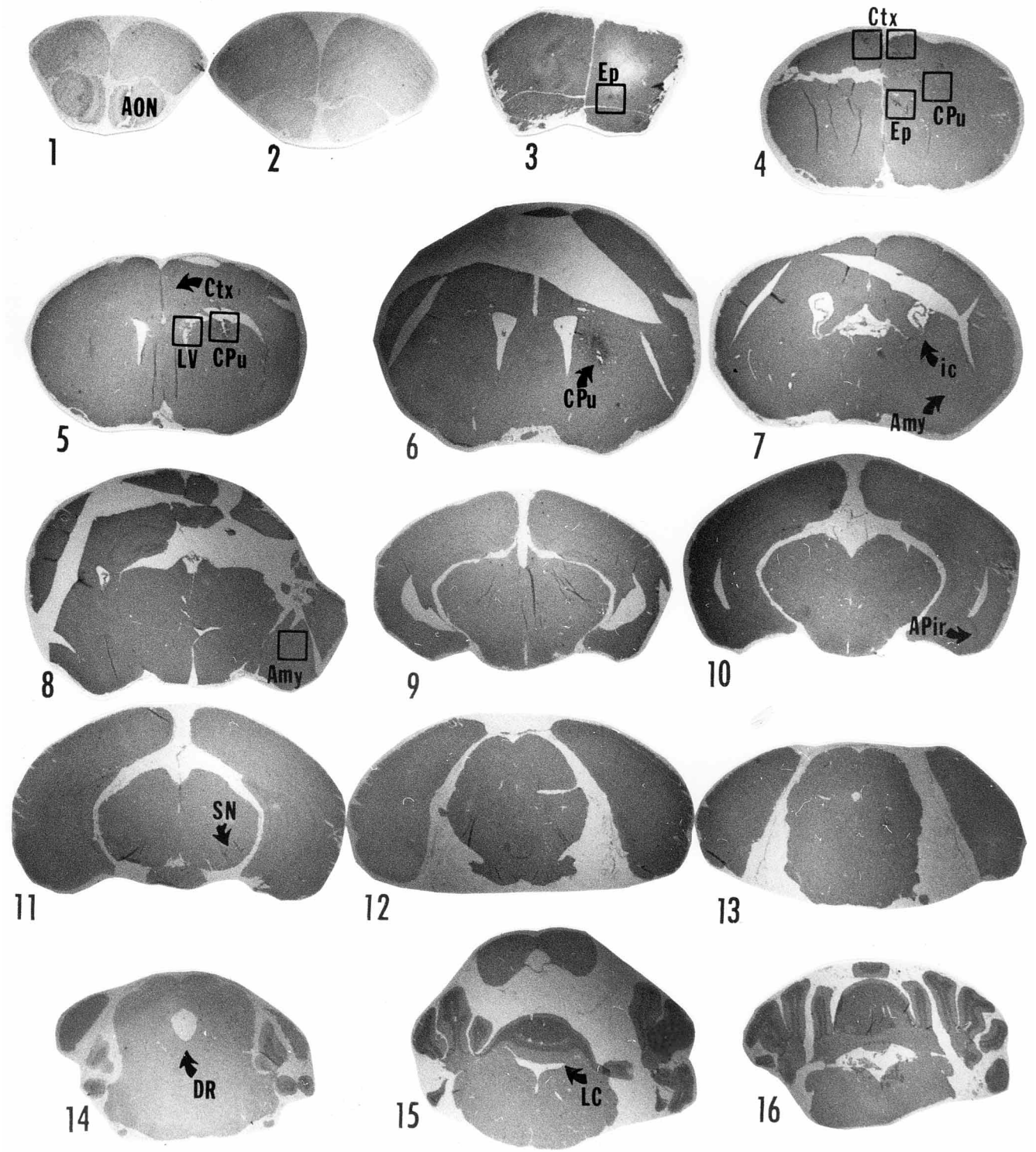

FIG. 2. Photograph of low-power-laser-scanned microscopic images of transverse sections through the brain of a mouse (52) harvested 5 days after injection of R3616 and processed as described in Materials and Methods. Sections 1 to 16 illustrate, in a rostral-to-caudal progression, representative sections from the levels of the brain subjected to HSV immunohistochemical analysis and counterstained with hematoxylin. Sections are separated by approximately 400 μm (range: 320 to 480 μm). The arrows and squares identify the locations of HSV-infected cells. Color photomicrographs of regions indicated by the arrows are shown at higher magnifications in Fig. 3 and 4. The center of the injection site is indicated by the arrow in the right caudate/putamen (CPu) in section 6 (see also Fig. 3b and c), whereas associated damage extends within the rostral caudate/putamen into sections 4 and 5 as indicated by the rightmost square in each section. These regions appear to be part of the needle track which is not in the plane of the section. In sections 3 to 6, ependymal cells (Ep) of the right lateral ventricle (LV) were also infected (ventral region, left squares). Outside the caudate/putamen, the majority of infected cells were found ipsilaterally in sections 4 and 5 in the motor and cingulate cortices, respectively (Ctx; top squares and arrows; see also Fig. 3k), in sections 7 and 8 in the amygdala (Amy; bottom arrow and square; see also Fig. 3l and 4g and k to m), and in section 10 in the amygdalopiriform transition area (APir; arrow; see also Fig. 3i and j). Fewer infected cells were located in the anterior olfactory nucleus (AON; section 1), in the contralateral motor cortex (Ctx; leftmost square in section 4), internal capsule (ic; top arrow in section 7; see also Fig. 3l), substantia nigra (SN; arrow in section 11; see also Fig. 4e and f), and locus coeruleus (LC; arrow in section 15; see also Fig. 4a and b). The arrow in section 14 indicates the location of the dorsal raphe (DR), which contains HSV-immunolabeled cells, in the brains of mice harvested on days 3 and 7 (see Fig. 4c and d).

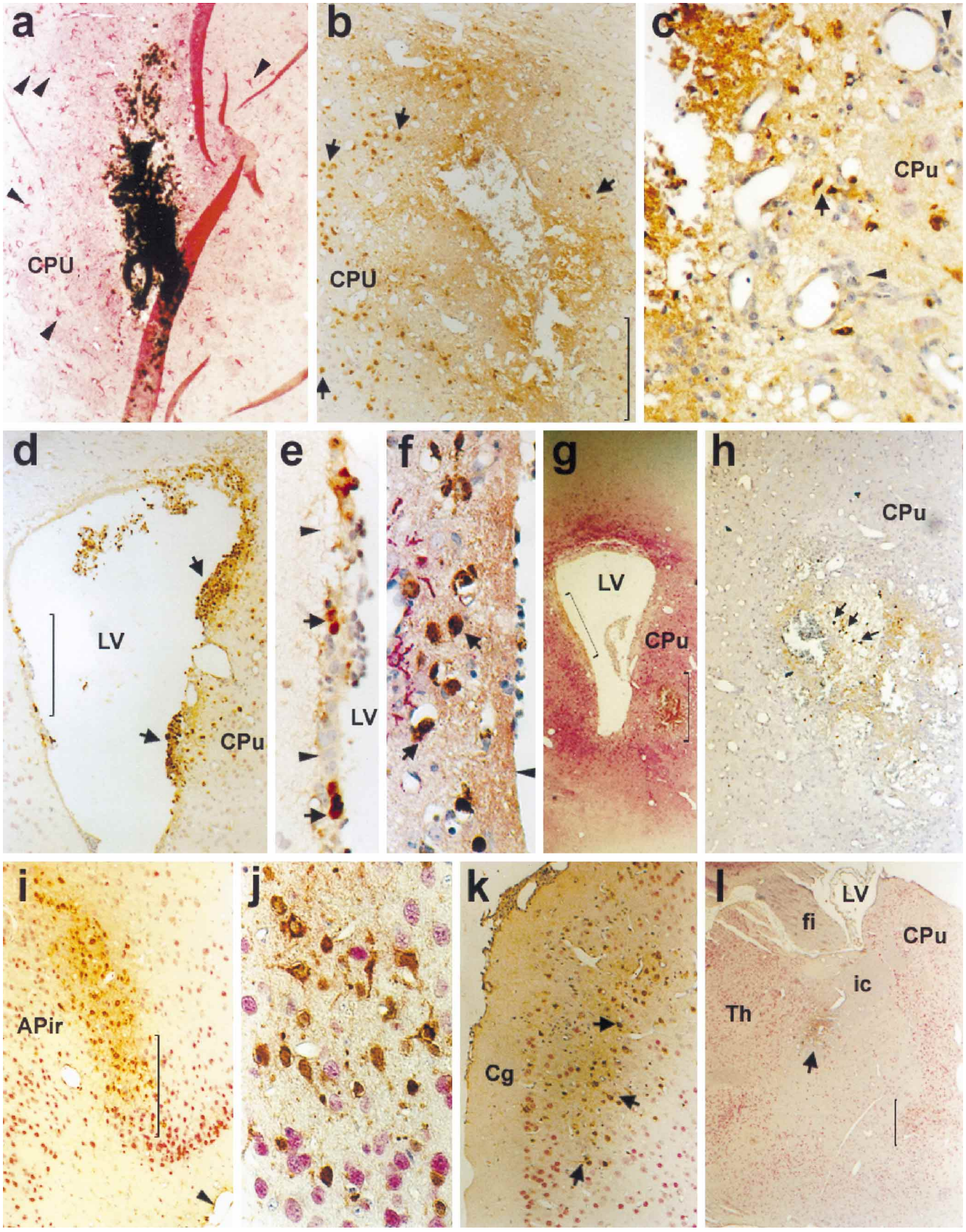

FIG. 3. Photomicrographs of representative fields of transverse sections through the brains of mice injected with a marking suspension (a) or R3616 recombinant virus (b to l). All panels show regions ipsilateral to the injection site (right side). Sections shown were immunolabeled with antibody to HSV alone (h) or with antibody to HSV and antibodies to astrocytes (anti-GFAP; panels a, f, and g) or neurons (A60; panels b to e and i to l). Viral antigens reacting with the antibody were colored

to the ventricles in the day 7 mouse or that R3616 replicated in the ependymal cells and progeny virus released into the CSF infected other cells. The latter argument is supported by the increase in the number of infected cells found in regions adjacent to the ventricles. Thus, the number of infected cells in the lateral septal nuclei (Fig. 3f; Table 1) and fimbria (bilaterally; data not shown and Table 1) at 7 days after infection was much higher than that found in these regions in the brains harvested on day 3 or 5 after infection. The small number of infected cells found in the dorsal raphe, locus coeruleus, substantia nigra, and contralateral motor cortex, etc., could be due to a combination of factors, including a small variation in injection site location.

Identity of infected cells. The types of cells infected both at the site of injection and at a more distant site were determined by a double-labeling technique in which sections were labeled successively with two antibodies, that is, anti-HSV and antiproteins specific for neurons, astrocytes, or oligodendrocytes (Fig. 4h to m), as described in Materials and Methods.

Microscopic studies of the sections containing infected cells led to two conclusions: (i) Infection and expression of viral antigens do not appear to be cell type specific inasmuch as cells immunopositive for HSV antigens were also found to be immunopositive for neuron-, astrocyte-, or oligodendrocyte-specific antibodies. Photomicrographs of double-immunostained sections taken near the injection site (Fig. 4h to j) or through the amygdala (Fig. 4k to m) from the brain of the day 5 mouse illustrate that infected neurons (Fig. 4h and k), astrocytes (Fig. 4i and l), and oligodendrocytes (Fig. 4j and m) were present in sites adjacent to the injection and at more distal sites. (ii) R3616 may be capable of limited, low-level replication in neurons in the mouse CNS. This conclusion rests on the observations that astrocytes and oligodendrocytes (Fig. 4l and m), in addition to neurons (Fig. 4k), were infected at sites distant to the site of infection. The rationale for this conclusion is that while it is reasonable to presume that neurons in distant nuclei could have become infected through their projections to or through the site of injection, as discussed earlier, such a mechanism cannot explain the infection of astrocytes or oligodendrocytes in these nuclei since these cell types do not have processes which project far from their cell bodies. One reasonable hypothesis to explain the infection of these glial cells is to propose that R3616 replicates in the nuclei of neurons which project to, but are distant from, the injection site. Progeny virus released from infected neurons in this distant site could then infect neighboring cells, neurons, or glial cells and thus could be responsible for the infection of astrocytes and oligodendrocytes in regions distal to the injection site.

DISCUSSION

The mouse is a useful model of human CNS infection with HSV, and studies on the replication and spread of wild-type HSV-1 strains in murine CNS abound (4, 16, 17, 30, 33, 34, 36, 38, 42, 43, 50, 52, 59, 63, 65). The fundamental observations are that wild-type strains of HSV rapidly spread from the site of infection to distant regions of the CNS and that the quantities of virus which can be recovered from the brain of a moribund mouse are vastly greater than the minimal lethal dose of the virus. The key features of wild-type virus infection are therefore the capacity to replicate at the site of injection, spread rapidly throughout the brain, and destroy the CNS.

HSV-1 contains at least 84 different genes of which as many as 45 are dispensable for replication in at least some cells in culture (56). Mutants with a deletion in one or more of many of these dispensable genes frequently exhibit excellent growth in some cell lines in vitro and a decrease in at least one if not both markers of virulence: capacity to invade the CNS from peripheral sites and capacity to multiply in the CNS after direct inoculation (6, 9, 13, 16, 20, 21, 37, 46, 47, 58, 66, 67). Measured on the basis of the minimal amounts of virus required for lethal infection of mice by the intracerebral route, the $\gamma_1$34.5$^-$ recombinants are among the least virulent, replication-competent mutants known. The central question, therefore, was whether the virus infected and destroyed CNS cells and whether the attenuation phenotype of the virus could be due to an altered host range. The emphasis of the experimental design of this study was to map as precisely as current methodology permits the distribution of infected cells in the CNS and the identity of the infected cells.

Our studies indicate the following: (i) The $\gamma_1$34.5$^-$ mutant R3616 infected and caused the destruction of cells predomi-

brown, whereas those reacting with cellular markers stained red. Sections in all panels were counterstained with hematoxylin. (a) Site of injection into neostriatum with a marking suspension on day 3 after injection. Arrowheads point to a few of the many astrocytes expressing GFAP in tissue surrounding the site of injection. Cells on the contralateral side did not react with this antibody (data not shown). The HSV antibody did not react with cells in these sections. (b and c) Site of R3616 injection into the neostriatum on day 5 after infection. The region indicated by the bracket in panel b is shown at higher magnification in panel c. The brown-staining cells in panel b (a few identified by arrows) and the diffuse matter surrounding these cells contain R3616 antigens. HSV-infected cells were present in intact regions of the neostriatum (b) at various distances (arrows) from the injection site. Closer to the injection site, the morphology of infected cells was difficult to determine. Visible at higher magnification (c) were the infected cells (two identified by an arrow) and the onset of perivascular cuffing—hematoxylin-stained cells surrounding the lumina of capillaries (arrowheads). (d and e) Right lateral ventricle (LV) at the level of the injection site illustrating the infected ependymal cell layer of the LV (a few identified by arrows). Panel d shows prominent HSV immunolabeling of regions of the multicellular ependymal layer (arrows). The medial ventricular ependymal cell layer within the bracket is shown at higher magnification in panel e. Panel e shows uninfected hematoxylin-stained ependymal cells lining the ventricles (lower arrowhead) that were in the same layer as comparably sized HSV-infected cells (arrows). The beginning of a separation of the infected ependymal layer from the adjacent brain tissue (top arrowhead) portended the disappearance of the ependymal layer in mice sacrificed on day 7 (panels f and g). (f) Photomicrograph of the medial border of the LV in the mouse sacrificed on day 7. The absence of an intact ependymal cell layer (arrowhead) was striking in comparison to that shown in panel e. Further from the surface of the LV, infected cells of the lateral septal nuclei (two identified by arrows) are visible. (g) Photomicrograph of the LV and injection site of the mouse sacrificed on day 7. The area shown in panel f is indicated by the left bracket, whereas the right bracket indicates the ventral region of the injection site shown in panel h. (h) The injection site 7 days after inoculation. Comparatively few HSV-immunostained cells were visible (arrows), the cell loss (indicated by an increased number of vacuoles) was greater, and HSV-immunostained cells were not visible at various distances from the injection site (as in panels b and c). (i) R3616-infected cells within the amygdalopiriform transition area in the temporal lobe of the cortex. This region is oriented here from top left to lower right. The portion of this region indicated by the bracket is shown at higher magnification in panel j. The arrowhead indicates the ventrolateral surface of the brain. (j) The neuronal morphology of many infected cells in the amygdalopiriform transition area was evident at a higher magnification. (k) A few of the many HSV-infected cells in this section, colored brown, of the cingulate cortex are identified by arrows. (l) Low-power magnification of the medial portion of a section through the level of the thalamus and the caudal portion of the neostriatum. Indicated by the arrow is a region of HSV-immunostained cells in the internal capsule, a fiber tract composed of axonal projections to and from cortical cells which pass through the caudate/putamen. The infected region shown abutted, but did not seem to include, the reticular thalamic nucleus just to the left. No infected cells were observed in other regions of the thalamus. The region indicated by the lower right bracket contained infected cells of the amygdala, shown at higher magnifications in Fig. 4, panel g and panels k to m. Although this region of the amygdala borders the ventrocaudal region of the neostriatum, the infected cells in this region were confined to this nucleus and were not observed elsewhere (e.g., the ventral region of the neostriatum). Abbreviations: CPU, caudate/putamen; APir, amygdalopiriform transition area; Cg, cingulate cortex; Th, thalamus; ic, internal capsule; fi, fimbria.

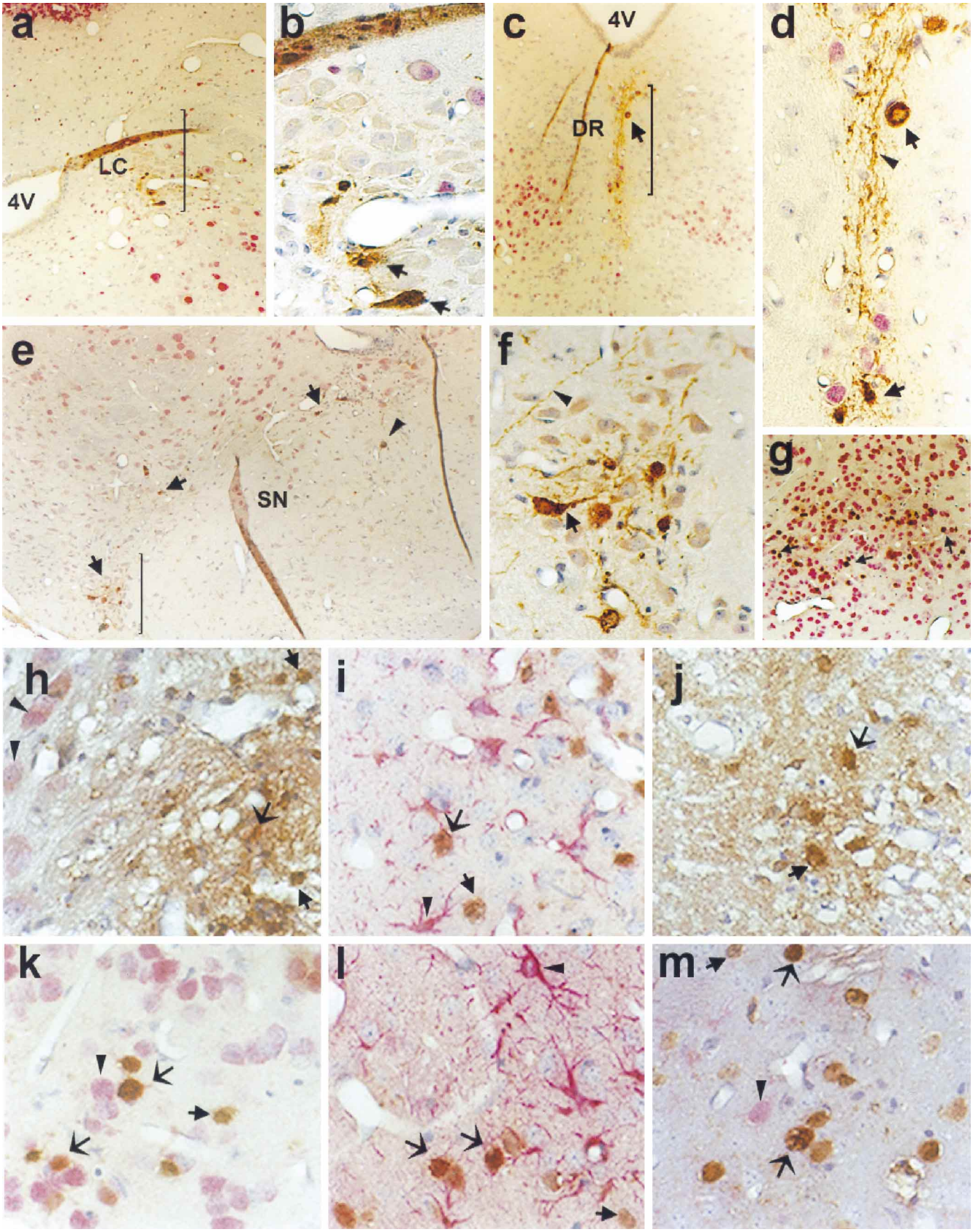

FIG. 4. Photomicrographs of representative fields of transverse sections through the brains of mice injected with R3616 virus. All panels show regions ipsilateral to the injection site (right side) with the exception of panels c and d, which show the midline. Sections shown were immunolabeled with antibody to HSV and with antibody to either neurons (A60; panels a to h and k), astrocytes (anti-GFAP; panels i and l), or oligodendrocytes (anti-S100; panels j and m). Viral antigens reacting

nantly at the site of injection. Given the small volume of the inoculum (1 μl), the concentration of virus was the highest at this site, and hence it is conceivable that some of the effects observed at this site represent the results of a high multiplicity of infection. (ii) Virus spread from the site of infection within the CNS to distant sites predominantly through axonal transport and in part through the CSF within the cerebral ventricles. As reported, following wild-type HSV-1 injection into lateral ventricles, infected cells are detected bilaterally in the piriform cortex, raphe nuclei, locus coeruleus, cerebral cortex, and septal nuclei (45). In our studies, with the exception of cells in the lateral septal nuclei and fimbria (addressed in Results) and a few cells in the contralateral motor cortex (consistent with spread through axonal transport), HSV-immunostained cells were confined to the ipsilateral hemisphere. This distribution of infected cells is consistent with retrograde spread of the virus along axons projecting to the neostriatum (40, 41, 44). (iii) R3616 did not discriminate against neurons, astrocytes, oligodendrocytes, or ependymal cells with respect to the capacity of these cells to become infected or, as far as we can assess, to synthesize and accumulate viral proteins. At the same time, infected cells were not detected in other regions of the CNS known to project to the caudate/putamen (e.g., several thalamic nuclei, other cortical regions, and the entopeduncular nucleus) (22, 27, 31). The absence of infected cells in these regions is due either to the lack of direct connections from these regions to the specific portion of the caudate/putamen inoculated or to the lack of susceptibility to infection with this mutant. In addition, while some regions containing HSV-immunolabeled cells both receive projections from and send projections to the caudate/putamen, the globus pallidus and the reticular nucleus of the substantia nigra only receive projections from cells of the caudate/putamen. Inasmuch as no infected cells were observed in this region of the forebrain and only one infected cell was observed in the reticular nucleus of the substantia nigra, the overwhelming absence of infected cells in these regions suggests that R3616 is transported in the retrograde direction. (iv) The recombinant R3616 may have replicated to a low level sufficient to spread to a small number of astrocytes and oligodendrocytes from neurons originally infected through projections to the site of inoculation. (v) Infection had run its course between day 5 and day 7 after infection. This conclusion is based on the observation that the number of cells infected with R3616 peaked near day 5 and that infected cells were being efficiently cleared from the CNS by day 7.

From these studies it is apparent that R3616 recombinant virus shares with wild-type viruses three properties, that is, ability to infect a variety of cells, retrograde transport in CNS neurons, and destruction of the infected cells. R3616, the $\gamma_1$34.5$^-$ virus, differs from wild-type virus in having reduced capacity to replicate in the CNS, as reflected both in the very small amounts of virus recovered from the brain (13) and in the inability to spread effectively from cell to cell.

CNS cells are generally highly susceptible to HSV-1 infection. The basis for the failure of the $\gamma_1$34.5$^-$ virus to multiply efficiently in the CNS is not clear. The immunoreactivity of the infected cells with the polyclonal antibodies to HSV suggests that infected cells make viral structural proteins, and hence the lack of infectious progeny portends a blocked event late in infection.

In contrast to the events occurring in normal mouse brain, R3616 does replicate well in malignant glioma cells (2) and is effective in destroying these cells when administered at the same time or 5 days after implantation of the glioma cells into the CNS of mice (5, 11). These observations suggest the possibility that the ability of $\gamma_1$34.5$^-$ virus to replicate hinges on the availability of factors associated with cell division rather than on cell origin.

The studies described in this report raise the question of the meaning of the term "neurovirulent" and, conversely, of the absolute meaning of the term "nonneurovirulent". In principle, the term neurovirulent describes an agent in gross biological terms and means that it causes disease by invading and multiplying in the brain. In more recent years, the term neurovirulent has also been applied inappropriately to agents which lack neuroinvasiveness but which will, if forced into the brain, multiply and cause disease. Hence, in the strictest sense, a neurovirulent virus is one which possesses the attributes of neuroinvasiveness and neurogrowth. The issues at the cellular level are quite different since viruses may prefer to replicate and destroy a specific type of cell in preference to another. If the end result, however, is disease and death, cell preferences qualify, but do not alter the basic neurovirulent properties of the virus.

It is the nonneurovirulent phenotype that is the most troublesome to define since it has no defined point compared to neurovirulence, which may be deduced from symptoms of morbidity and confirmed by immunohistochemical analysis. $\gamma_1$34.5 mutants lack the attributes of neuroinvasiveness and neurogrowth. They do not lack the property of being destructive to the cells under conditions that have not been defined but that are presumed to include exposure of high numbers of virus particles per cell. It seems intuitively clear that the death of 10^6 cells in properly selected domains of a mouse brain is not likely to result in morbidity but that the death of a thousand times

with the antibody were colored brown, whereas those reacting with cellular markers were colored red. Sections in all panels were counterstained with hematoxylin. (a and b) HSV-infected cells in the locus coeruleus. The region indicated by the bracket in panel a is shown at a higher magnification in panel b. In panel b, the intact morphology of one infected neuronal cell is evident (lower arrow), whereas the integrity and nature of other immunostained cells (upper arrow) or cell debris in this region were unclear. (c and d) Immunostained cells (arrows) and fibers (arrowhead) in the dorsal raphe of the mouse sacrificed on day 3. The bracketed region of the dorsal raphe in panel c and the cell identified by the arrow are shown at a higher magnification in panel d. (e) HSV-infected cells of the substantia nigra (SN) in several regions of the compact nucleus (arrows), as well as one HSV-labeled cell in the reticular nucleus (arrowhead). Panel f shows a higher magnification of the SN indicated by the bracket in panel e. The immunostained fibers (arrowhead) and neuronal morphology of one of several infected cells (arrow) were evident. (g) A few of the many infected cells of the amygdala are indicated here by arrows. Sections adjacent to this one were reacted with both the anti-HSV antibody and one of the antibodies specific for cell type and are shown at a higher magnification in panels k to m below. (h to m) Photomicrographs of sections adjacent to the injection site (panels h to j) and through the amygdala (panels k to m) of an R3616-infected mouse. In all panels, cells double labeled with HSV and cell-type-specific antibody are indicated by a broad arrow. Cells immunopositive for HSV antigens are indicated by normal arrows, while cells immunostained by the cell-type-specific marker only are indicated by arrowheads. (h to j) Near the injection site, cells immunopositive for cell-type-specific antibodies were often difficult to identify against the dark background of diffuse viral protein or heavily HSV-immunolabeled cells. Shown are regions at the injection site (panel h) or along the border of the injection site (panels i and j). (k to m) In the amygdala, double-labeled cells were more amenable to identification. In panel k, the red nuclear staining of the A60 (neuronal) antibody was readily demonstrable beneath the largely nuclear staining of the HSV antibody. The neuronal morphology of one double-labeled neuron (upper broad arrow) was revealed by the immunostaining of part of the neuronal process. In panel l, cytoplasmic immunostaining with anti-GFAP antibody revealed the typical morphology of astrocytic processes while leaving the nuclei in the plane of the section unstained (arrowhead). The double labeling of infected astrocytes (broad arrows) was often easy to detect. Panel m shows that, while largely a cytoplasmic stain, the S-100 antibody revealed the soma of an S-100-labeled cell (arrowhead) and of S-100 and HSV double-immunolabeled cells (arrows). Elsewhere in the panel, S-100 antibody revealed the myelin sheath of axonal fibers formed by oligodendrocytes. Abbreviations: LC, locus coeruleus; DR, dorsal raphe nucleus; 4V, fourth ventricle.

TABLE 1. Distribution of R3616-infected cells in infected mouse brains

Location[a]	No. of infected cells[b] at day:		
	3	5	7
Injection site	>30	>30	11–30
Caudate/putamen (neostriatum)	>30	>30	0
Anterior olfactory nucleus	0	1–5	NA[c]
Amygdala	11–30	>30	>30
Amygdalopiriform transition area	11–30	>30	0 (NA)
Cingulate and motor cortices	0	>30	0
Motor cortex (contralateral)	0	1–5	0
Internal capsule	0	>30	0
Substantia nigra	0	6–10	0
Dorsal raphe nucleus	6–10	0	1–5
Locus coeruleus	1–5	1–5	NA
Lateral septal nuclei	1–5	0	11–30
Fimbria, ipsilateral	6–10	0	11–30
Fimbria, contralateral	0	0	>30
Ventricular ependymal layer	>30	>30	1–5

[a] Ipsilateral nucleus unless specified.
[b] Maximum number per section.
[c] NA, a portion of the potentially relevant section was missing.

that number may be lethal. Given these problems, lack of neurovirulence is seen to be a relative term which can be measured by determining the virus dose which causes morbidity assuming that the virus was delivered initially to a nonlethal CNS site, or by defining virus spread, the spectrum of infected cells exhibiting morbidity, and the viral products made in CNS cells. In critical situations in which virulence must be defined in operational terms, the latter procedure is both preferable and necessary.

ACKNOWLEDGMENTS

We thank Lindsay Smith, Ginny Zagaja, and Sogol Jahedi for technical assistance.

N.S.M. is a postdoctoral fellow of the National Alliance for Research on Schizophrenia and Depression (N.A.R.S.A.D.). These studies were aided by grants from the National Cancer Institute (CA47451) and the United States Public Health Service.

REFERENCES

1. **Ackermann, M., D. K. Braun, L. Pereira, and B. Roizman.** 1984. Characterization of α proteins 0, 4, and 27 with monoclonal antibodies. J. Virol. **52:**108–118.
2. **Advani, S., P. Song, G. Sibley, Y. Kataok, B. Roizman, and R. R. Weichselbaum.** Unpublished data.
3. **Alheid, G. F., J. S. de Olmos, and C. A. Beltramino.** 1995. Amygdala and extended amgydala, p. 495–578. *In* G. Paxinos (ed.), The rat nervous system, 2nd ed. Academic Press, San Diego, Calif.
4. **Anderson, J. R., and H. J. Field.** 1983. The distribution of herpes simplex type I antigen in mouse central nervous system after different routes of inoculation. J. Neurol. Sci. **60:**181–195.
5. **Andreansky, S. S., B. He, Y. Gilespie, L. Soroceanu, J. Markert, B. Roizman, and R. J. Whitley.** 1996. The application of genetically engineered herpes simplex viruses to the treatment of experimental animal tumors. Proc. Natl. Acad. Sci. USA **93:**11313–11318.
6. **Balan, P., N. Davis-Poynter, S. Bell, H. Atkinson, H. Browne, and T. Minson.** 1994. An analysis of the in vitro and in vivo phenotypes of mutants of herpes simplex virus type 1 lacking glycoproteins gG, gE, gI or the putative gJ. J. Gen. Virol. **75:**1245–1258.
7. **Barnett, E., M. D. Cassell, and S. Perlman.** 1993. Two neurotropic viruses, herpes simplex virus type 1 and mouse hepatitis virus, spread along different neural pathways from the main olfactory bulb. Neuroscience **57:**1007–1025.
8. **Barnett, E. M., G. D. Evans, N. Sun, S. Perlman, and M. D. Cassell.** 1995. Anterograde tracing of trigeminal afferent pathways from the murine tooth pulp to cortex using herpes simplex virus type 1. J. Neurosci. **15:**2972–2984.
9. **Ben-Hur, T., Y. Asher, E. Tabor, G. Darai, and Y. Becker.** 1987. HSV-1 virulence for mice by the intracerebral route is encoded by the BamHI-L DNA fragment containing the cell fusion gene. Arch. Virol. **96:**117–122.
10. **Boerman, R. H., A. Mitro, B. R. Bloem, E. P. Arnoldus, A. K. Raap, A. C. Peters, and M. van der Ploeg.** 1991. Detection of herpes simplex virus in the ependyma of experimentally infected mice. Acta Virol. **35:**450–457.
11. **Chambers, R., G. Y. Gillespie, L. Soroceanu, S. Andreansky, S. Chatterjee, J. Chou, B. Roizman, and R. J. Whitley.** 1995. Comparison of genetically engineered herpes simplex viruses for the treatment of brain tumors in a *scid* mouse model of human malignant glioma. Proc. Natl. Acad. Sci. USA **92:** 1411–1415.
12. **Chou, J., J. Chen, M. Gross, and B. Roizman.** 1995. Association of a M_r 90,000 phosphoprotein with protein kinase PKR in cells exhibiting enhanced phosphorylation of translation initiation factor eIF-2α and premature shutoff of protein synthesis after infection with $\gamma_1 34.5^-$ mutants of herpes simplex virus 1. Proc. Natl. Acad. Sci. USA **92:**10516–10520.
13. **Chou, J., E. R. Kern, R. J. Whitley, and B. Roizman.** 1990. Mapping of herpes simplex virus-1 neurovirulence to $\gamma_1 34.5$, a gene nonessential for growth in culture. Science **250:**1262–1266.
14. **Chou, J., A. P. W. Poon, J. Johnson, and B. Roizman.** 1994. Differential response of human cells to deletions and stop codons in the $\gamma_1 34.5$ gene of herpes simplex virus. J. Virol. **68:**8304–8311.
15. **Chou, J., and B. Roizman.** 1992. The $\gamma_1 34.5$ gene of herpes simplex virus 1 precludes neuroblastoma cells from triggering total shutoff of protein synthesis characteristic of programmed cell death in neuronal cells. Proc. Natl. Acad. Sci. USA **89:**3266–3270.
16. **Chrisp, C. E., J. C. Sunstrum, D. R. Averill, Jr., M. Levine, and J. C. Glorioso.** 1989. Characterization of encephalitis in adult mice induced by intracerebral inoculation of herpes simplex virus type 1 (KOS) and comparison with mutants showing decreased virulence. Lab. Invest. **60:**822–830.
17. **Cook, M. L., and J. G. Stevens.** 1973. Pathogenesis of herpetic neuritis and ganglionitis in mice: evidence for intra-axonal transport of infection. Infect. Immun. **7:**272–288.
18. **Ejercito, P. M., E. D. Kieff, and B. R. Roizman.** 1968. Characterization of herpes simplex virus differing in their effect on social behavior of infected cells. J. Gen. Virol. **2:**357–364.
19. **Fallon, J. H., and S. E. Loughlin.** 1995. Substantia nigra, p. 215–237. *In* G. Paxinos (ed.), The rat nervous system, 2nd ed. Academic Press, San Diego, Calif.
20. **Field, H. J., and G. Darby.** 1980. Pathogenicity in mice of strains of herpes simplex virus which are resistant to acyclovir in vitro and in vivo. Antimicrob. Agents Chemother. **17:**209–216.
21. **Field, H. J., and P. Wildy.** 1978. The pathogenesis of thymidine kinase deficient mutants of herpes simplex virus in mice. J. Hyg. Camb. **81:**267–277.
22. **Fink-Jensen, A., and J. D. Mikkelsen.** 1989. The striato-entopeduncular pathway in the rat. A retrograde transport study with wheat germ-agglutinin-horseradish peroxidase. Brain Res. **476:**194–198.
23. **Franklin, K. B. J., and G. Paxinos.** 1996. The mouse brain in stereotaxic coordinates. Academic Press, San Diego, Calif.
24. **Graybiel, A. M., and C. W. Ragsdale, Jr.** 1979. Fiber connections of the basal ganglia. Prog. Brain Res. **51:**239–283.
25. **He, B., J. Chou, D. A. Liebermann, B. Hoffman, and B. Roizman.** 1996. The carboxyl terminus of the murine MyD116 gene substitutes for the corresponding domain of the $\gamma_1 34.5$ gene of herpes simplex virus to preclude the premature shutoff of total protein synthesis in infected human cells. J. Virol. **70:**84–90.
26. **He, B., M. Gross, and B. Roizman.** 1997. The $\gamma_1 34.5$ protein of herpes simplex virus 1 complexes with protein phosphatase 1α to dephosphorylate the α subunit of the eIF-2 translation initiation factor and preclude the shutoff of protein synthesis by double stranded RNA activated protein kinase (PKR). Proc. Natl. Acad. Sci. USA **94:**843–848.
27. **Heimer, L., D. S. Aahm, and G. F. Alheid.** 1995. Basal ganglia, p. 579–628. *In* G. Paxinos (ed.), The rat nervous system, 2nd ed. Academic Press, San Diego.
28. **Hersh, S. M., and E. L. White.** 1982. A quantitative study of the thalamocortical and other synapses in layer IV of pyramidal cells projecting from mouse SmI cortex to the caudate-putamen nucleus. J. Comp. Neurol. **211:** 217–225.
29. **Hill, T. J., H. J. Field, and A. P. C. Roome.** 1972. Intra-axonal location of herpes simplex particles. J. Gen. Virol. **15:**253–255.
30. **Johnson, R. T.** 1964. The pathogenesis of herpes virus encephalitis. Part 1. Virus pathways to the nervous system of suckling mice demonstrated by fluorescent antibody staining. J. Exp. Med. **119:**343–356.
31. **Jones, E. G., and R. Y. Leavitt.** 1974. Retrograde axonal transport and the demonstration of non-specific projections to the cerebral cortex and striatum from thalamic intralaminar nuclei in the rat, cat and monkey. J. Comp. Neurol. **154:**349–378.
32. **Kita, H., and S. T. Kitai.** 1990. Amygdaloid projections to the frontal cortex and the striatum in the rat. J. Comp. Neurol. **298:**40–49.
33. **Knotts, F. B., M. L. Cook, and J. G. Stevens.** 1974. Pathogenesis of herpetic encephalitis in mice after ophthalmic inoculation. J. Infect. Dis. **130:**16–27.
34. **Kristensson, K., I. Nennesmo, L. Persson, and E. Lycke.** 1982. Neuron to neuron transmission of herpes simplex virus: transport of virus from skin to brainstem nuclei. J. Neurol. Sci. **54:**149–156.
35. **Kristensson, K., E. Lycke, and J. Sjöstrand** 1971. Spread of herpes simplex

virus in peripheral nerves. Acta Neuropathol. (Berlin) **17:**44–53.
36. **Lascano, E. F., and M. I. Berria.** 1980. Histological study of the progression of herpes simplex virus in mice. Arch. Virol. **64:**67–79.
37. **MacLean, A. R., M. ul-Fareed, L. Robertson, J. Harland, and S. M. Brown.** 1991. Herpes simplex virus type 1 deletion variants 1714 and 1716 pinpoint neurovirulence-related sequences in Glasgow strain 17+ between immediate early gene 1 and the 'a' sequence. J. Gen. Virol. **72:**631–639.
38. **Martin, J. R., F. J. Jenkins, and D. B. Henken.** 1991. Targets of herpes simplex virus type 1 infection in a mouse corneal model. Acta Neuropathol. **82:**353–363.
39. **Mattiace, L. A., M. D. Baring, K. F. Manaye, G. A. Mihailoff, and D. C. German.** 1989. Mesostriatal projections in BALB/c and CBA mice: a quantitative retrograde neuroanatomical tracing study. Brain Res. Bull. **23:**61–68.
40. **McDonald, A. J.** 1991. Organization of amygdaloid projections to the prefrontal cortex and associated striatum in the rat. Neuroscience **44:**1–14.
41. **McDonald, A. J.** 1991. Topographical organization of amygdaloid projections to the caudatoputamen, nucleus accumbens, and related striatal-like areas of the rat brain. Neuroscience **44:**15–33.
42. **McFarland, D. J., and J. Hotchin.** 1987. Contrasting patterns of virus spread and neuropathology following microinjection of herpes simplex virus into the hippocampus or cerebellum of mice. J. Neurol. Sci. **79:**255–265.
43. **McFarland, D. J., E. Sikora, and J. Hotchin.** 1986. The production of focal herpes encephalitis in mice by stereotaxic inoculation of virus: anatomical and behavioral effects. J. Neurol. Sci. **72:**307–318.
44. **McGeorge, A. J., and R. L. M. Faull.** 1989. The organization of the projection from the cerebral cortex to the striatum in the rat. Neuroscience **29:**503–537.
45. **McLean, J. H., M. T. Shipley, and D. I. Bernstein.** 1989. Golgi-like, transneuronal retrograde labelling with CNS injections of herpes simplex virus type 1. Brain. Res. Bull. **22:**867–881.
46. **Meignier, B., R. Longnecker, P. Mavromara-Nazos, A. E. Sears, and B. Roizman.** 1988. Virulence of latency by genetically engineered deletion mutants of herpes simplex virus 1. Virology **162:**251–254.
47. **Meignier, B., R. Longnecker, and B. Roizman.** 1988. In vivo behavior of genetically engineered herpes simplex viruses R7017 and R7020: construction and evaluation in rodents. J. Infect. Dis. **158:**602–614.
48. **Merkel, K. H., and M. Zimmer.** 1981. Herpes simplex encephalitis. A modified indirect immunoperoxidase technique for rapid diagnosis in paraffin-embedded tissue. Arch. Pathol. Lab. Med. **105:**351–352.
49. **Mitro, A., and M. Palkovits.** 1981. The morphology of the rat brain ventricles, ependyma, and periventricular structures. Bibl. Anat. **21:**1–110.
50. **Mizota, A., R. D. Dix, and D. I. Hamasaki.** 1993. Bilateral electroretinographic changes induced by unilateral intra-visual cortex inoculation of herpes simplex virus type 1 in BALB/c mice. Doc. Ophthalmol. **84:**213–230.
51. **Mullen, R. J., C. R. Buck, and A. M. Smith.** 1992. NeuN, a neuronal specific nuclear protein in vertebrates. Development **116:**201–211.
52. **Neeley, S. P., A. J. Cross, T. J. Crow, J. A. Johnson, and G. R. Taylor.** 1985. Herpes simplex virus encephalitis: neuroanatomical and neurochemical selectivity. J. Neurol. Sci. **71:**325–337.
53. **Perlman, S., E. Barnett, and G. Jacobsen.** 1993. Mouse hepatitis virus and herpes simplex virus move along different CNS pathways. Adv. Exp. Med. Biol. **342:**313–318.
54. **Poon, A. P. W., and B. Roizman.** Differentiation of the shutoff of protein synthesis by virion host shutoff and mutant $\gamma_1$34.5 genes of herpes simplex virus 1. Virology, in press.
55. **Porter, L. L., and E. L. White.** 1983. Afferent and efferent pathways of the vibrissal regions of primary motor cortex in the mouse. J. Comp. Neurol. **214:**279–289.
56. **Roizman, B.** 1996. The function of herpes simplex virus genes: a primer for genetic engineering of novel vectors. Proc. Natl. Acad. Sci. USA **93:**11307–11312.
57. **Roller, R. J., and B. Roizman.** 1991. Herpes simplex virus I RNA binding protein U_S11 negatively regulates the accumulation of a truncated viral mRNA. J. Virol. **65:**5873–5879.
58. **Sears, A. E., I. W. Halliburton, B. Meignier, S. Silver, and B. Roizman.** 1985. Herpes simplex virus 1 mutant deleted in the α22 gene: growth and gene expression in permissive and restrictive cells and establishment of latency in mice. J. Virol. **55:**338–346.
59. **Seegal, R. F., and D. J. McFarland.** 1988. Stereotaxic microinjection of HSV-1 selectively decreases striatal dopamine concentrations in mice. Brain Res. **445:**234–240.
60. **Steindler, D. A., L. G. Isaacson, and B. K. Trosko.** 1983. Combined immunocytochemistry and autoradiographic retrograde axonal tracing for identification of transmitters of projection neurons. J. Neurosci. Methods **9:**217–228.
61. **Taha, M. Y., G. B. Clements, and S. M. Brown.** 1989. A variant of herpes simplex virus type 2 strain HG52 with a 1.5 Kb deletion in R_L between 0 to 0.02 and 0.81 to 0.83 map units is non-neurovirulent in mice. J. Gen. Virol. **70:**705–716.
62. **Taha, M. Y., G. B. Clements, and S. M. Brown.** 1989. The herpes simplex virus type 2 (HG52) variant JH2604 has a 1488 bp deletion which eliminates neurovirulence in mice. J. Gen. Virol. **70:**3073–3078.
63. **Tomlinson, A. H., and M. M. Esiri.** 1983. Herpes simplex encephalitis: immunohistological demonstration of spread via olfactory pathways in mice. J. Neurol. Sci. **60:**473–484.
64. **Vann, V. R., and S. S. Atherton.** 1991. Neural spread of herpes simplex virus after anterior chamber inoculation. Invest. Opthalmol. Vis. Sci. **32:**2462–2472.
65. **Webb, S. J., R. P. Eglin, M. Reading, and M. M. Esiri.** 1989. Experimental murine herpes simplex encephalitis: immunohistochemical detection of virus antigens. Neuropathol. Appl. Neurobiol. **15:**165–174.
66. **Whitley, R. J., E. R. Kern, S. Chatterjee, J. Chou, and B. Roizman.** 1993. Replication, establishment of latency, and induced reactivation of herpes simplex virus $\gamma_1$34.5$^-$ deletion mutants in rodent models. J. Clin. Invest. **91:**2837–2844.
66a. **Whitley, R. J., E. Kern, J. Chou, and B. Roizman.** Unpublished data.
66b. **Whitley, R. J., E. Kern, B. He, and B. Roizman.** Unpublished data.
67. **Yamada, Y., H. Kimura, T. Morishima, T. Daikoku, K. Maeno, and Y. Nishiyama.** 1991. The pathogenicity of ribonucleotide reductase-null mutants of herpes simplex virus type 1 in mice. J. Infect. Dis. **164:**1091–1097.